

RESIN SATURATION EFFECT ON THE MECHANICAL BEHAVIOR OF CFRP LAMINATE PROCESSED BY RTM: QUASI-STATIC LOAD

Marcos Yutaka Shiino, marcosshiino@yahoo.com.br

Maria Odila Hilário Cioffi, cioffi@feg.unesp.br

Herman Jacobus Cornelis Voorwald, voorwald@feg.unesp.br

UNESP – Univ. Estadual Paulista, Campus Guaratinguetá, Fatigue and Aeronautical Materials Research Group-DMT/FEG/UNESP, Av. Ariberto Pereira da Cunha, 333-CEP12516-410, Guaratinguetá/SP-Brasil

Abstract. Resin Transfer Moulding (RTM) has been largely employed in the structural parts of the aircraft. The method allows the production of complex parts with high fiber volume percentage and low content of voids. Nonetheless, care must be taken in the mold conception, as a poor quality project can carry out to defects, such as dry spots. Another feature that has demonstrated some concern in the part quality is the resin saturation phenomena, which degree is a function of time. This is an unavoidable phenomena that can be reduced by displacing the inlet gates at the strategic positions. This research work is focused on the influence of the resin saturation degree in the final mechanical properties of the laminate. The mold design, one line inlet gate, easily provided a laminate with two distinct regions of saturation level that was detected by an ultrasonic C-scan inspection. The mechanical behaviour was evaluated in uniaxial tensile test that may provide different results from these two regions. Comparison between the attenuation level from C-scan map with tensile strength showed some influence of the saturation degree, as tensile test loads the tows, in which have major role in the saturation process.

Keywords: Resin Transfer Moulding (RTM), carbon fiber reinforced polymer (CFRP), tensile test, non-destructive test (NDT)

1. INTRODUCTION

RTM process has been largely employed in the aeronautical field mainly for producing structural components, which demand for high fiber volume percentage usually greater than 40% (Aduriz et. al., 2006). The injection process can be performed by multiple inlet and outlet ports that usually have strategic positions in the mold to avoid voids and entrapped air, common defects in the process. The low viscosity resin (<500 mPa.s) flows through the dry preform within a closed rigid mold, the time of this procedure depends on the fiber volume percentage, in which also dictates the mechanical performance (Mattson et. al., 2007; Pearce et. al., 1997).

This process uses thermoset resins with long pot life to ensure complete filling of the mold prior to the gelling time. An isothermal temperature is involved for epoxy resin during the polymerization (Ruiz and Trochu, 2005).

One can choose between constant pressure, which conducts to a pressure gradient as far as from the inlet gate (injection point), or constant flow rate (varied pressure) (Zhou et. al., 2007).

The discussed process has mainly been used for fabrics, which are fibers bundled into tows and woven or stitched into different architectures. The scenario presented so far, one can infer that resin can flow through two sizes of pore medium: one within the fiber tows that form pores in the range of 1-10 μm , and pores of millimeters formed by fiber tows that cross each other. The called micropore slowly saturates, in the meanwhile the flow front quickly advances through inter-tows (macropore). Saturation degree of the intra-tow pore is dependent of time as demonstrated in Eq. (1) (Zhou et. al., 2007; Garcia et. al., 2010; Gourichon et. al., 2005).

$$\frac{K}{\mu} \nabla p = \phi \frac{\partial S}{\partial t} \quad (1)$$

The first expression, left hand side, describes the resin flow by Darcy's law, and on the right hand side is the saturation rate.

Where K is the permeability, μ is the fluid viscosity, ∇p is pressure gradient, ϕ is the porosity and S the saturation degree.

As the tow impregnation is dependent of time, using long mold the difference in resin saturation between the two opposite sides of the mold will be high. Besides, in cases of high fiber volume content the microscopic flow affects the overall flow (Amico and Lekakou, 2001) in addition to variation of the preform compaction that influences the resin content (Bayldon and Daniel, 2009). In ultrasonic inspection the aspect of the C-scan map is a concern due to the differences in attenuation signal.

Quality inspection in laminates processed by RTM with characteristics of low attenuation signal close to the inlet gate has not been reported. For a better comprehension of the differences in attenuation signal along the C-scan map, tensile tests and fractographic observations were carried out.

2. MATERIAL AND METHODS

2.1. Materials and process

The laminate was processed with a stacking sequence of 5 multidirectional non-crimp fabric (NCF) stitched in the following sequence: [90/-45/0/45]. The fiber bundles were stitched with a polyester yarn (PE 80DTex) in the chain pattern. Those plies were assembled to form a quasi-isotropic laminate that provided approximately a 54% in fiber volume fraction. The summary of the fiber properties used in the fabric is shown in Tab. 1.

Table 1. Fabric properties

Fabric	Fiber type	Weight (g/m ²)	Fiber tow (x1000)
90°/-45°/0°/45°	IMS	580	24

One line inlet gate combined with one vacuum gate at the end of a rectangular rigid mold was used to produce the laminate plate. The CYCOM 890 low viscosity resin, provided by CYTEC, was injected at 100 °C, which did not transfer heat through the walls due to the heated line as well as the heated mold, in order to keep the viscosity at 75 mPa.s.

A constant pressure of 3.4 bar was measured inside the mold as seen in Fig. 1. In the end of the injection process, the resin ran through the outlet vacuum pipe for some time to assure that the remaining bubbles were removed. Afterwards, the cure cycle took place at 180 °C during 120 minutes.

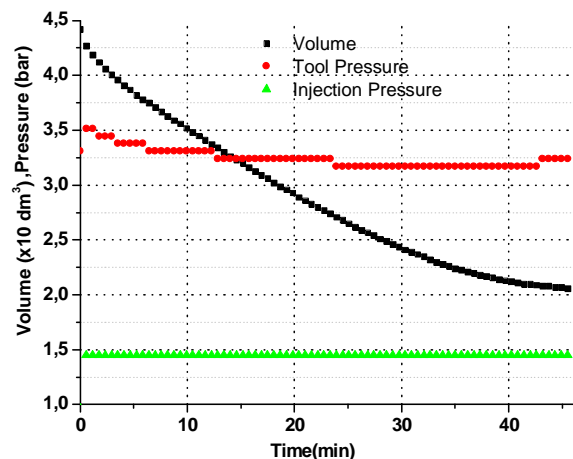


Figure 1. Injection progress in laminate NCF

2.2. Ultrasonic test

The ultrasonic inspection was performed by an MUIS32 equipment from MATEC company, which works in a pulse-echo mode. The equipment is equipped with a water bath, as a coupling medium, and the specific probe for a thin laminate can range between 5 to 10MH. For a quasi-isotropic laminate the 10MHz flat probe worked out to detect all the features that influences the performance of a composite material, e.g. dry spots, race-tracking, and fiber misalignment.

Firstly the A-scan graphic aided in calibrating the patterns of a typical structural composite peaks (reference), and then captured all the peaks, in gates 1 and 2, in which work as acquisition data, the difference between the pattern peaks (without defects) and more attenuated peaks are shown in a gray scale C-scan map, for which can be attributed a color scale for a better evaluation. The resulting analysis of the background echo, data achieved from Gate 2, is sufficient to provide an accurate assessment of the laminate health.

Fig. 2 represents the color scale of attenuation signal that is employed along the analysis of the C-scan maps, where 0% represents low attenuation or region of low material density, which is proportional to acoustic impedance, as shown in Eq. (2), and 100% all the sound returned, which means there is a region without void, or high material density.



Figure 2. Color scale for C-scan maps

$$z = \rho c \quad (2)$$

Where z is the acoustic impedance, ρ is the material density, and c the sound velocity.

2.3. Tensile test

The tensile tests was performed in accordance with ASTM D3039, in which the tensile strength (F_x) was used to compare the different attenuation regions, as shown in Fig. 3. A 100 kN load cell was set to use in the ISTRON 8801 servo-hydraulic testing machine with a speed test of 2mm/min. The coupons were tested without tabs but the failure site was assured in the gauge section.

The coupons 3, 9 and 21 were taken from the low attenuation region, and the specimens 14, 16, 19, 22 and 23 were taken from the high attenuation region. Each rectangle (175×25) mm² represents one coupon and the middle line of the plate separates the two regions. In Fig. 3, all coupons were cut from a plate with (300×400) mm² in the same processing conditions.

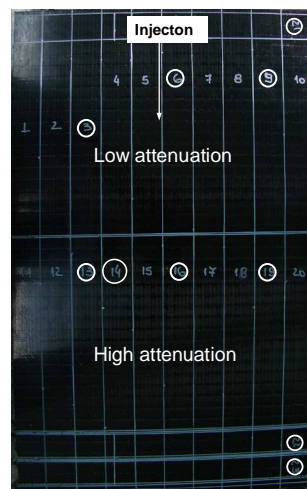


Figure 3. NCF laminate plate

2.4. Fractography

JEOL JSM5310 Scanning Electron Microscopy (SEM) was performed with a tungsten filament working at 15 keV.

Parameters were set in the way to obtain large number of secondary electrons, due to the concern about topographic information. The analysed coupons were coated by a gold thin layer in order to increase the electron conductivity of the fractured composite, a film with less than 20 nm thickness is recommended to avoid the misinterpretation of the topography.

This procedure was conducted to have an overall understanding of the fracture pattern between two hypothetical far different values in the same attenuation region, such as happened between specimens 14 and 16.

3. RESULTS AND DISCUSSION

3.1. Ultrasonic inspection

In Fig. 4, the attenuation tends to increase in the way to the outlet vacuum gate, and it is clearly the resin path in green color attenuation, around 60%. The low attenuation, closed to the inlet gate, may be associated to the long time of resin exposure. As a result the fiber tows became saturated and scattering losses were reduced. Other sources of energy loss came from the interface between the plies.

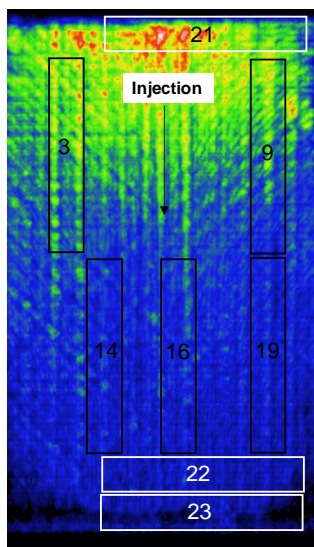


Figure 4. C-scan map of NCF laminate

The half end of the laminate has the attenuation around 80%, separating the laminate into two distinct regions as defined in section 2.3: low attenuation and high attenuation.

In black attenuation color, at the corners in Fig. 4, is considered defects introduced during the injection procedure, as the flow front pressure lowered due to the mold length and vacuum influence.

3.2. Tensile test

In Table 2 a trend in the average by attenuation region, and the dispersion of the results pointed out an influence of the resin saturation degree. The mentioned trend can lead to a misinterpretation as this dispersion may be related to a natural distribution of the fiber tensile strength (Shiino, 2011). For a better understand, a sketch in Fig. 5 was set to show this influence.

Table 2. Tensile test results of NCF laminate

Attenuation region	Coupon number	Tensile strength (MPa)	Average by attenuation region (MPa)	Overall average (MPa)
Low attenuation	21	738	745 ± 20	733 ± 31
	3	767		
	9	729		
High attenuation	14	700	725 ± 36	
	16	778		
	19	701		
	22	699		
	23	750		

Analyzing each coupon in Fig. 5, coupons 16 and 23 have outstanding values, considering the high attenuation signal in blue color. In coupons 3 and 21 a predominant low attenuation in green color is present, which contributed to increase the average.

Due to the high value obtained from specimen 23, within the high attenuation field, the hypothesis of the resin saturation into the fiber tows that could increase the tensile strength may be considered weak, despite the fact that 3 specimens within 5 tested specimens showed some evidence of low performance in the considered degree of resin saturation. From this point, it is considered safe to say, based on the limited data available, that the different regions in the C-scan map did not affect the composite performance under uniaxial tensile test.

In regard to the low values obtained from specimens 14, 19 and 22, this may be attributed to inhomogeneities along the cross section of the tested specimen, e.g. resin-rich regions.

To clarify the overall picture stated in this section, fractographic analysis was conducted.

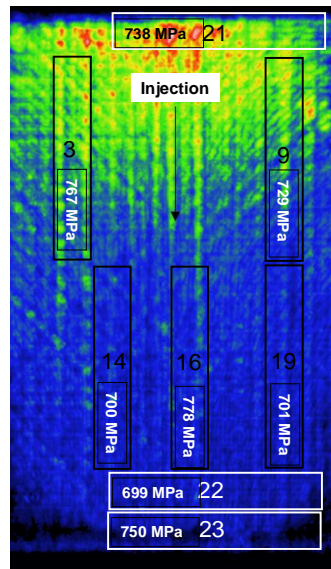


Figure 5. C-scan map of NCF laminate

3.3. Fractography

Fig. 6 illustrates intraply resin-rich region, depicted in rectangle, that may have contributed to decrease the specimen performance. These regions were predominant in this coupon, and could be defined as linear vacancies, which are flaws introduced during the fabric manufacturing process.

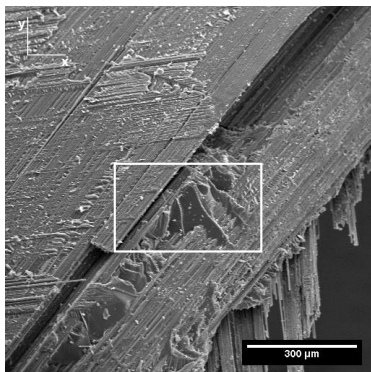


Figure 6. Intraply resin in specimen 14 – 100x

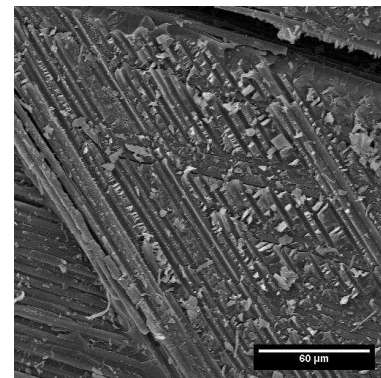


Figure 7. Interlaminar fracture in specimen 16 – 500x

More homogeneous fractures were observed in coupon 16 as illustrated in Fig.7, which shows hackles along the interlaminar fracture. Strong interface was observed in both analysed coupons, like process of pull-out and clean fiber were not present.

4. CONCLUSION

Despite the fact that the low attenuation signal is very sharp in the inlet gate, the consequences, regarding mechanical performance in tensile test, demonstrated a poor relationship. The fractographic analysis showed an influence of flaws that might be associated with the dispersive results. Therefore the 400 mm length mold did not cause enough influence in the intratow impregnation domain on static mechanical properties of a quasi-isotropic laminate.

So far impregnation of the fiber tows in tensile test can be considered worthless in applications of static load. Further analysis will be necessary for a better evaluation of the resin saturation degree in dynamic application.

5. ACKNOWLEDGEMENTS

The authors acknowledge the financial assistance of FAPESP by process numbers 2009/04123-4 and 2006/02121-6.

6. REFERENCES

- Aduriz, X.A., Lupi, C., Baileul, J.L., Sobotka, V., Luduc, D., Boyard, N., Leferve, N., Le Bozec, C. Chapeleau, X., Delaunay, X., Boisrobert, C., 2006, "Fibre Optics Sensors Applied to Resin Transfer Moulding (RTM) in Aeronautic: Composite Materials Process Optimization", Proceedings of SPIE - The International Society for Optical Engineering, pp.6189.
- Amico, S., Lekakou, C., 2001, "An experimental study of the permeability and capillarity pressure in resin-transfer moulding", Composites Science and Technology, Vol.61, pp.1945-1959.
- Bayldon, J.M., Daniel, I.M., 2009, "Flow modeling of the VARTM process including resin saturation effects", Composites: Part A, Vol. 40, pp.1044-1052.
- García, J.A., Gascón, Ll., Chinesta, F., 2010, "A flux limiter strategy for solving the saturation equation in RTM process simulation", Composites: Part A, Vol.41, pp.78-82.
- Gourichon, B., Binetruy, C., Krawczack, P., 2005, "Experimental investigation of high fiber tow count fabric unsaturation during RTM", Composites Science and Technology, Vol.66, pp.976-982.
- Mattson, D., Joffe, R., Varna, J., 2007, "Methodology for Characterization of Internal Structures Parameters Governing Performance in NCF Composites", Composites Part B: Engineering, Vol.38, pp.44-57.
- Pearce, N., Guild, F., Summerscales, J., 1997, "A study of effects of convergent flow fronts on the properties of fibre reinforced composites produced by RTM", Composites Part A, Vol.29A, pp. 141-152.
- Ruiz, D., Trochu, F., 2005, "Numerical analysis of cure temperature and internal stresses in the thin and thick RTM parts", Composites: Part A, Vol.36, pp.806-826.
- Shiino, M.Y., 2011, "Desenvolvimento e caracterização de compósitos processados por RTM para aplicação aeroespacial", Dissertação de Mestrado, Universidade Estadual Paulista-UNESP, Guaratinguetá-SP, Brasil, 97p.
- Zhou, F., Alms, J., Advani, S.G., 2007, "A closed form solution for low in dual scale fibrous porous media under constant injection pressure conditions" Composites Science and Technology, Vol.68, pp.699-708.